Paper submitted to the 4th Miami International Symposium on Multi-Phase Transport & Particulate Phenomena, Miami Beach, FL, December 15-17, 1986.

EFFECT OF BOILING REGIME ON MELT STREAM BREAKUP IN WATER*

by

B. W. Spencer, J. D. Gabor, and J. C. Cassulo

Reactor Analysis and Safety Division
Argonne National Laboratory
9700 South Cass Avenue
Argonne, IL 60439

CONF-861204--6

DE87 004705

*Work sponsored by Electric Power Research Institute and U.S. Nuclear Regulatory Commission.

EFFECT OF BOILING REGIME ON MELT STREAM BREAKUP IN WATER

B. W. Spencer, J. D. Gabor, and J. C. Cassulo
Reactor Analysis and Safety Division
Argonne National Laboratory
9700 South Cass Avenue
Argonne, IL 60439

ABSTRACT

A study has been performed examining the breakup and mixing behavior of an initially coherent stream of high-density melt as it flows downward through water. This work has application to the quenching of molten core materials as they drain downward during a postulated severe reactor accident. The study has included examination of various models of breakup distances based upon interfacial instabilities dominated either by liquid-liquid contact or by liquid-vapor contact. A series of experiments was performed to provide a data base for assessment of the various modeling approaches. The experiments involved Wood's metal (T_m = 73°C, ρ = 9.2 g/cm^3, d_j = 20 mm) poured into a deep pool of water. The temperature of the water and Wood's metal were varied to span the range from single-phase, liquid-liquid contact to the film boiling regime. Experiment results showed that breakup occurred largely as a result of the spreading and entrainment from the leading edge of the jet. However, for streams of sufficient lengths a breakup length could be discerned at which there was no longer a coherent central core of the jet to feed the leading edge region. The erosion of the vertical trailing column is by Kelvin-Helmholtz instabilities and related disengagement of droplets from the jet into the surrounding fluid. For conditions of liquid-liquid contact, the breakup length has been found to be about 20 jet diameters; when substantial vapor is produced at the interface due to heat transfer from the jet to the water, the breakup distance was found to range to as high as 50 jet diameters. The former values are close to the analytical prediction of Taylor, whereas the latter values are better predicted by the model of Epstein and Fauske.

INTRODUCTION

Studies have been under way at Argonne National Laboratory (ANL) and elsewhere to investigate the phenomena of a severe core melt accident in a light water reactor (LWR). These studies are motivated in part by our need to understand the accident at TMI-2 as well as continuing need in general to understand the risks of a severe accident. Recent studies at ANL have focused on two broad aspects of a core melt accident, namely: 1) effects of the flow of molten core materials (corium) into the reactor pressure vessel (RPV) lower head region,[1,2] and 2) effects of the flow of corium through a breach in the RPV lower head into the reactor cavity or pedestal region below.[3] For the in-vessel case it is likely that water will be present initially in the RPV lower head region; however, the presence of water beneath the vessel depends upon both the accident sequence and upon the containment design. The presence of water in these regions has important influences on the course of an accident, and its merit remains a topic of some controversy. We have been investigating the effect of water on the quench of corium (including steam pressure buildup and possible steam explosion), the character of the corium debris following interaction with water, the coolability of that debris given a continuing presence of water, the

erosion of substrate materials such as steel (in-vessel) and concrete (ex-vessel), dispersion of corium debris owing to rapid steam generation and sweep-out, and hydrogen generation owing to oxidation of metallic constituents of the corium during interaction with water.

A fundamental aspect of these processes is the breakup of the corium as it falls through the water and its intermixing with the water.[4-6] There has been extensive study of large coherent melt masses entering water, particularly in the context of steam explosions. Recent work at ANL, however, has focused on what we regard as a more probable mode of corium entry into water, i.e., relatively small diameter pour streams or rivulets. In-vessel, this has three possible origins. First, materials having low melting temperature but high melt superheat, such as the Ag-In-Cd control rod material used in many reactors, will likely flow downward through intact fuel rod channels, thereby entering the water as small rivulets. Later, if the accident progresses to a stage of significant liquifaction of core materials, these core materials will freeze during the downward melt migration, forming temporary crusts (analogous to self-crucible formation). Although one can only speculate, it is likely that the crust failure mode, if any, would be by cracking or local meltouts so that downward corium flow would resume by streams or sheets rather than a large coherent mass. Finally, even if there were coherent release of a large melt mass, its downward motion would be impeded by the massive lower internal structure. Starting with the bottom caps of the fuel assemblies, there exists a number of such barriers including the core support plate, core support forging, and various flow distribution plates. The downward flowing melt mass would be intercepted by the structures and would be redistributed into individual streams pouring through the available openings in the plates. Similarly, if an accident progresses to a stage in which the bottom head is breached, the mode of breach may involve meltout of weld stubs, control assembly housings, or other local failures, and in these cases the corium will exit the vessel as a stream rather than a coherent large melt mass. (Of course, in-vessel flow is driven by gravity-head drainage whereas flow from the vessel is driven by the prevailing vessel-to-containment pressure difference.) Hence the mode of contact between corium and water and the ensuing events are of generic interest in arriving at best-estimate assessments of accident progression, both in-vessel and ex-vessel.

A key aspect of the corium-water interaction is the large corium-to-water heat flux during the transient period that the jet flows through the water. The corium temperature is predicted to range from 2300 to 2700C, far into the film boiling regime, and because of this very high corium temperature the heat flux is expected to exceed even the peak nucleate boiling heat flux albeit there being film boiling. The effect of this high heat flux insofar as flow regime and steam generation are concerned depends upon the subcooling of the water. If the water is at or near the saturation temperature for the existing pressure, as is typically the case in-vessel, the corium-to-water heat transfer will cause copius steam generation. The water pool into which the corium is entering will experience an abrupt agitation as the steam is formed in the vicinity of the jet. For the reactor cases of interest, the water pool is typically large in lateral dimension compared to the diameter of a single jet. The steam which forms surrounding the jet typically coalesces into large bubbles which rise to the surface in the region surrounding the jet. Of course, a lateral component of water velocity is also established owing to the sudden volumetric growth in the jet/vapor region. The global behavior is considerably more complex if the size of the jet is not small in relation to the pool diameter, or if there is an array of jets flowing into the water over a large cross-sectional area. Then the steam cannot so readily escape upward through the region of the downflowing jet(s), and water may tend to be pushed downward ahead of the melt (if there is a low restriction outlet near the bottom), or in extreme cases the water may be forced to flow upward through the melt region, displaced by the jet and steam

volume. The latter case of forced corium/water intermixing may be more relevant to some experiment configurations than to reactor cases, however.

In the foregoing the water was considered to be at or near its saturation temperature so that corium quench took place through net steam generation. For those cases where the water is adequately subcooled, most likely ex-vessel cases where the reactor cavity or pedestal region is flooded, the steam is largely condensed locally in the water pool and the agitation or boilup of the pool remains minimal. This offers the possibility to quench the molten core materials without concern for steam overpressurization in the containment plus the possibility of forming a coolable debris bed at the base given the continued availability of water. This technique has been used commercially to quench molten slag from a coal-fired boiler into easily handled though relatively large fragment sizes.

We are presently investigating certain basic issues which characterize the corium jet behavior, namely, the quench rate, the jet breakup distance, the distance to assure formation of a particle bed (requires solidification during the fall stage), and the debris characteristics. Briefly, the significance of these issues in the reactor system is as follows:

Quench rate: The quench rate is determined in large part by the jet surface area. Hence, the quench rate is normally enhanced by increasing the surface area through breakup into sheets and droplets owing to hydrodynamic instabilities. Counteracting this, however, high rates of steam formation may limit the intermixing between the jet material and the water such that the high density melt, particularly that in the trailing column behind the jet leading edge, may flow through a region of high void fraction, lessening both the breakup of the column (as opposed to the leading edge) as well as the overall quench rate. This is particularly important if the water is at or near saturation temperature.

Jet breakup distance: The breakup behavior of a corium jet under in-vessel or ex-vessel conditions of interest (ignoring capillary or atomization breakup) depends largely on the density of the ambient fluid. The jet breakup owing to hydrodynamic instabilities is far slower in a steam or gaseous environment than in water. Since the jet flow through water may itself create a locally high void fraction region, the dominating influence of the water vs the steam becomes somewhat unclear, and this has a large effect on the prediction of breakup distance. Previous work has demonstrated that the breakup occurs both at the leading edge (Raleigh-Taylor instability) and along the trailing column (Kelvin-Helmholz and possibly other instabilities).[2] The jet breakup is regarded as complete at a distance into the water where there is no longer a central core or continuum of melt to feed material into the leading edge; i.e., at a distance beyond which there is only an assemblage of downward flowing droplets or particles. At this point there is no longer leading edge breakup per se (although there may be spreading of the particle field). The distance of flow through the water to arrive at complete breakup is determined solely by the breakup behavior along the trailing, nominally vertical column. It is important to know this distance not only for modeling the jet breakup and quench rate behavior, but also for predicting the impingement heat flux if there is an intervening surface to intercept the downward flowing jet.

Solidification distance: An important feature of the corium quench is that at some point the corium will begin to solidify. When this begins depends in large part on the amount of "melt superheat" in the corium. The melt superheat is defined here as the excess temperature above the freezing temperature. In cases of small melt superheat, solidification may begin

quickly and impede the instability-related breakup process. In tests in our laboratory not involving reactor-material corium, we have observed this competition between jet breakup and freezing and have found cases where freezing occurred so rapidly that breakup was inhibited.[2] The result was frozen sheets and porous clinkers of relatively large size which, because of large voidage, would be readily coolable as a bed of heat-generating debris. If solidifcation is delayed and largely follows the breakup process, there remains an assemblage of droplets which will continue to transfer heat as they fall through the water. If well behaved, the freezing begins at the outer surface and progresses inward in the droplets. In corium quench tests in very deep water pools (melt superheat $\tilde{}$ 160K), we have found an abundance of spherical-shaped particles in the 1-10 mm size range, many of which were broken hollow shells.[1] The debris also appeared to include broken shell segments. Here we define the solidification distance as the distance traveled through the water at which a bed of discrete particles would be formed if collected upon a surface without the significant presence of melt to "cement" the particles and render the region impermeable to water.

Debris characterization. The coolability of a heat-generating debris bed depends on certain characteristic features such as the representative size of particles, the spread in the size distribution, the shapes, bed voidage, and bed depth, among other parameters.

Objective

To address these issues there has been a program of both reactor-material and simulant-material jet flow quench studies and related analyses at ANL involving collaboration between EPRI and USNRC (RES). The specific work described here involved a series of simulant-material tests performed in a transparent apparatus so that the breakup behavior of a dense jet in water could be photographed. These tests were performed under geometric conditions very similar to the reactor material tests. The specific objectives were to characterize the breakup behavior of the jet using the transparent apparatus, to examine the effect of boiling regime on jet breakup (i.e., especially the effect of varying intensity of steam generation), and to characterize the debris formed from the interaction.

Approach

All the tests described here involved the gravity-head pour of a single melt stream into a deep vessel of water. In these tests the lateral dimension of the water pool was selected to be large in relation to the jet diameter so that two-dimensional mixing would be achieved, unimpeded by the presence of nearby boundaries; the depth of the pool was selected to exceed the solidification depth. Since the jet-to-ambient fluid density ratio is the principal parameter affecting jet breakup under the conditions of interest, a relatively high density melt was sought. In early tests, Wood's metal was used. Although satisfactory in most regards, it had the drawback that its freezing temperature is below the normal boiling point of water. This prevented examination of solidified debris for cases in which the water temperature was close to the saturation temperature. (All tests were performed at one atmosphere pressure.) In later tests Cerrotru was used so that the debris froze even in saturated water. The initial temperatures of the melts ranged up to 450C so that the boiling regime was close to if not actually in film boiling. At present there has been no attempt to go to higher temperature where film boiling is certain due to concern for possible vapor explosion damaging the apparatus. No vapor explosions have occurred in our reactor material tests in this contact mode, however.

EXPERIMENT DESCRIPTION

The jet breakup tests were conducted in the apparatus shown in Fig. 1. It consisted of sections of 6-in. (152.4-mm ID) Pyrex pipe joined together by flanges. The water was heated by nichrome strip heaters attached to the external wall of the Pyrex column. The melt furnace/injector was mounted on top of the Pyrex column. Injection was initiated by a solenoid valve pressurizing a gas cylinder driving a circular cutter through a 0.05-mm stainless steel diaphragm. (The slide gate shown in Fig. 1 was not used in these tests.) The diaphragm was pressed against the tube wall by the cylindrical cutter, assuring it was removed from the path of the melt. The melt flowed through the inside of the cutter cylinder and through the inside of the delivery tube. The melt delivery tube was 25 mm ID for the Wood's metal (WM) tests and 20 mm ID for the Cerrotru (CT) tests, and extended to 30 cm above the water surface. The cover gas was either air or steam, although previous scoping tests had shown that the selection of cover gas had little effect on the jet behavior following the first few jet diameters of flow through the water.[2] All tests were performed with the system vented through a trap seal to atmospheric pressure at the top. This prevented the buildup of high steam pressure in the apparatus during the test. The injector had nominally 3 psig pressure to assure smooth outflow of melt from the vessel as the vessel emptied.

The system was instrumented with thermocouples and pressure sensors. Small diameter, fast-response thermocouples were located at various elevations along the side of the water pool (Fig. 1) and at various elevations in the melt furnace. Strain gauge pressure transducers were located in the freeboard spaces of the water pool and melt injector, near the bottom of the water pool, and near the midplane of the water pool.

The thermocouples were monitored by a Doric Trendicator 400 A during the heatup phase. A Honeywell 101 magnetic tape unit and a Honeywell 1858 visicorder were used to record thermocouple and pressure transducer data during the tests. Weathermeasure and Shinho controllers were used for the melt furnace and Pyrex column heaters. Five Hycam cameras (Red Lake Laboratories) operated at 500 fps were used to obtain motion pictures of the event. Four cameras were focused to obtain localized views, and one camera photographed the entire column length.

EXPERIMENT CONDITIONS

The tests were performed both with Wood's metal and Cerrotru. Wood's metal is an alloy consisting of 50% bismuth, 25% lead, 12.5% tin, and 12.5% cadmium. It has a high density (9200 kg/m^3 at 100C) and a very low melting point (73C). Cerrotru (Cerro Metal Products, Bellefonte, PA) is a eutectic mixture of 58% bismuth and 42% tin. It also has a high density (8670 kg/m^3) and a low melting point (138C). Its advantage over Wood's metal for these tests is that it freezes in water at saturation temperature at 1 atm pressure, and hence the fragments solidify following breakup and could be examined.

The following conditions were maintained nominally constant for the series of tests described: the water pool depth was 1.46 m, the water pool inside diameter was 15.2 cm (6 in), the distance from the exit of the melt injection tube to the water surface was 15.2 cm (6 in), the melt drainage was by gravity head plus about 6.8 kPa gauge (3 psig), and the melt velocity upon entering the water was about 3 m/s. The nominal mass of Wood's metal was 2.0 kg. The Cerrotru tests, which utilized a larger size injector, used a mass of 6 kg for JWM-2 and 4 kg for JWM-5 and 6.

Test conditions for the jet breakup tests are summarized in Table 1. The cover gas was either air or steam in these tests. Steam was used to preclude the

TABLE 1. Summary of conditions for jet breakup tests

Test No.	Jet Matl	CG	$D_{j,i}$, mm	$T_{j,i}$, C	$T_{w,i}$, C	Notes
23	WM	air	20	125	-	Free jet fall through air
20	WM	air	22	100	24	Reference test
28	WM	steam	22	100	24	Condensable cover gas
7	WM	air	22	250	24	Effect of increased
32	WM	air	22	220	24	melt superheat
19	WM	air	22	110	100	Effect of net
29	WM	air	22	130	100	vapor generation
13	WM	air	22	250	100	(droplets not
24	WM	air	22	500	100	solidified
JWM-2	CT	steam	18	250	100	Solidification of
JWM-5	CT	steam	18	<150	100	fragments
JWM-6	CT	steam	11	<100	100	

WM = Wood's metal (T_m = 73C); melt delivery tube = 25 mm ID

CT = Cerrotru (T_m = 138C); melt delivery tube = 20 mm ID

entrainment of noncondensable gas into the water with the jet, despite the fact that previous scoping tests had indicated that the entrainment effect was limited to only the first few diameters of jet penetration (i.e., considerably shorter than the breakup distance). The jet diameter was measured as it entered the water using a motion picture analyzer. The value listed in Table 1 is a representative diameter during the time that the jet penetrated 20-30 diameters into the water. The jet diameter was usually quite regular in behavior during that time, although in some cases a few droplets or a small rivulet preceded the main flow by a small amount. Eventually the diameter of the stream reduced when the injector emptied; a smaller stream typically followed owing to drainage of the residual film from the injector wall. The measured jet diameters were used to reduce the penetration data.

RESULTS

A test was performed (#23) in which the Wood's metal (WM) was dropped through the apparatus without water present. This was to serve as a point of reference for jet flow velocity and breakup behavior in a completely gaseous environment in order to compare the behavior in a high void fraction steam/water mixture. The leading edge position of the jet is shown vs. time in Fig. 2. (All jet penetration distances have been normalized by the initial diameter of the jet.) The result shows that the jet accelerated in a regular manner under the influence of gravity in the low density ambient gas. The jet surface remained smooth over the visible fall distance of 0.8 m (L/D_j = 40). The diameter became smaller owing to the stretching out effect of the gravity acceleration, but the

capillary mode of breakup into droplets was not observed over the available distance although it would be expectd given a sufficiently long distance. This test merely confirmed the expected behavior; i.e., that a high density jet of the size and velocity of interest would experience negligible breakup in a gas/vapor environment in contrast, as will be seen, to the water environment.

Cases without Net Steam Generation

The first series of tests with water was performed with the water highly subcooled so that there was essentially no influence of net steam generation. Test #20 was the reference test with the jet temperature at the nominal water boiling point; test #23 was similar except that a steam (condensable) cover gas region was established replacing the air normally used; tests #7 and #32 used two different diameters and a higher temperature to attain local boiling at the jet/water interface. A dominant feature of all the tests performed was the sudden blunting and enlargement of the jet leading edge as it entered the water. The diameter increased by at least 2x, immediately as the leading edge broke through the water surface. This was the start of formation of the characteristic vortex ball at the leading edge which initially dominated the jet breakup. This behavior is depicted in Fig. 3. The effect of the sudden enlargement of the leading edge was to form a sizable pocket in its wake entraining cover gas into the water. This pocket was initially close to the same diameter as the newly formed vortex ball, ~ 2x the jet diameter. The pocket typically collapsed, and the water reflooded the cavity up to the surface by about 0.1 s. Thereafter there is thought to have been a small annulus of entrained cover gas (CG) as the jet column continued to enter the water, but it was not as obvious as the initial entrainment. Motion pictures showed that disengagement of droplets occurred from the leading edge, and that the disengaged droplets accumulated in the wake region of the vortex ball, spreading outward into the surrounding water. With no net steam generation, the motion picture view of the jet through the water was quite good, although the jet became somewhat obscured by the released bubbles of CG as well as the field of disengaged droplets. The droplets were much smaller than the jet diameter and hence settled at a much slower velocity through the water than did the central core jet region. Hence a growing field of droplets freezing into particles was being left behind in the surrounding water where they settled relatively slowly to the base. In this set of tests without net steam generation, the water pool remained quiescent throughout.

The breakup of the jet into disengaged droplets was observed to occur not only at the jet leading edge but also along the growing length of the trailing jet column. Surface irregularities formed along the column, grew in amplitude and ejected droplets from the column into the surrounding water. In some cases the irregularity appeared to be a ring that extended completely around the column, and the "bulge" would grow and emit droplets. This was especially evident in test #7 with the smaller diameter stream. Regularly spaced bulges appeared at ~ 13 mm intervals along the column in that test. It was evident from the motion pictures that much more breakup was taking place initially at the leading edge than along the trailing column. As the jet penetration into the water progressed, however, the surface area of the trailing column increased, and the loss of material from the column, albeit at a relatively slow rate, had an effect of depleting the mass in the column. A point was reached where the overall loss of material from the column consumed the column diameter, and hence there was no longer any central core of high velocity material to feed the vortex ball at the leading edge. At this point a quasi-static condition was established (assuming the jet flow didn't run out) which consisted of a central high-velocity continuum flow in the upper pool region undergoing mass depletion by droplet disengagement along the vertical melt/water interface. Beyond this, and surrounding this, there was a field of droplets/particles settling at slower velocity than the jet core velocity. The details of this could not be readily

discerned near the breakup length because of the density of surrounding disengaged droplets. However, this distance could be inferred from the penetration rate behavior of the leading edge, Fig. 2. The data shows two distinct penetration rates. Initially the leading edge penetrated at a velocity only about 20% less than the entrance velocity and remained quite constant. Later, there was a reduction in the leading edge penetration rate reflecting a new, slower velocity. The interpretation of this behavior is readily apparent with the aid of Fig. 3. As long as there was a high-velocity central core of melt feeding into the leading edge region, the penetration rate remained fast, reflective of the core velocity. However, when the core became fully depleted at the breakup distance, the leading edge flow merely reflected the gravity settling of the droplets/particles formed from the breakup.

From this behavior it is also apparent that there are two dominating modes of breakup; i.e., disengagement of liquid droplets into the wake of the vortex ball at the leading edge and the less spectacular appearing erosion of material from along the trailing column. The relative importance of these was examined in test #20. In that test the breakup length was about 20 L/D's. The velocity of the jet upon entry into the water was 2.7 m/s, the velocity of leading edge penetration was essentially constant at 2.1 m/s during the initial breakup stage, and the velocity of the trailing column feeding the leading edge was essentially the same as the entry velocity, 2.7 m/s. Using this net rate of influx of jet material into the leading edge plus the breakup length, one can crudely calculate that in the time needed to erode the jet radius along the trailing column (i.e., the time to reach the distance of complete breakup), there has been an influx of jet mass into the leading edge equivalent to about five jet L/D's. Hence, during the initial breakup stage of this test, about five times more mass was disengaged overall from the leading edge than from the trailing column. Of course, beyond that time all the breakup occurred along the vertical column since there no longer was a jet leading edge per se. It can be concluded from these observations that jet breakup in the melt/water system without appreciable steam generation is dominated by mass efflux from the leading edge vortex ball during the time the leading edge exists, and is dominated by mass efflux from the trailing vertical column during the quasi-steady period following, dependent upon the duration of the jet flow.

The penetration rate results in Fig. 2 show that tests #20 and 28 were almost identical, indicating no overall effect of entrainment of a condensable vs. noncondensable cover gas. The motion pictures showed formation of an entrainment pocket behind the leading edge upon jet entry into the water with the steam CG as was the case with the air. The steam pocket collapsed radially inward by condensation at about 0.06 s rather than the slower refill of the pocket with air. The void collapse by condensation did not have any noticeable effect on the jet column, however. Results of tests specifically examining this type of entrainment were presented previously.[2] Starting about L/D = 20, both sets of data show a slowing down of the leading edge, interpreted here as indicative of the breakup distance. Visual observation in the motion pictures also tends to support the notion that there is a loss of distinct central core feeding the vortex ball at about this penetration depth. Rather than an abrupt decrease in penetration velocity as the leading edge changes from high-velocity jet influx to particle settling, the decrease is seen to be gradual, probably indicating that particle interactions lessen as the particle field spreads laterally. The settling velocity becomes constant beyond L/D = 25 for these tests. For test #20, the constant settling velocity was found to be 0.82 m/s. If we assume that this is the terminal velocity for a single particle in an infinite medium, and furthermore assume a spherical particle shape, we estimate the particle size to be 2.8 mm diameter. This is somewhat smaller than the representative particle size of about 5 mm, although in fact most of the particles were oblong and

cluster-like rather than spherical and so would have a lower terminal velocity, in line with the measured value.

Companion tests #7 and 32 at higher melt temperature showed behavior very similar to one another, although the camera view for #7 did not extend deep enough into the pool to determine the breakup distance. With the highly subcooled water, there was no steam generation on a large enough scale to be observable in these tests. The penetration rate through the water was slightly faster than for tests #20 and 28. Based upon test #32, the breakup distance was about L/D = 25, somewhat longer than tests #20 and 28. With the larger melt superheat in these tests, the debris was generally smaller in size and consisted of more spherically shaped particles, representing perhaps a more complete hydrodynamic breakup before freezing at 140C melt superheat than in the other tests with 30C melt superheat. This is also reflected in the smaller terminal velocity.

Cases with Net Steam Generation

A set of four tests (19, 29, 13, and 24) was performed with increasing jet temperature with the water temperature increased to the boiling point. These tests were characterized by varying intensities of net steam generation. There was no solid debris formed at the 100C system temperature. The results showing the leading edge penetration rates into the water are given in Fig. 4. The penetration behavior was quite different than the tests without steam generation. In fact the penetration rates measured for tests #24 and 29 were comparable to test #23, the jet free fall through air (Fig. 2). The cameras were not aligned deep enough in the pool to capture the break point for tests #13 and 19. For test #29 the break occurred at L/D = 43; for test #24 there was no obvious break point in the viewable distance of L/D = 50. In viewing the motion pictures there were dramatic visible differences in the effect of the steam generation over the melt superheat range of these tests. In test #19 ($T_{j,i}$ = 115C, $T_{w,i}$ = 100C) there was relatively little steam formed and there was little resulting agitation in the pool. The steam bubbles in this series of tests accumulated around the jet, tending to obscure the jet behavior. However, this was minimal for the small ΔT conditions of test #19. Most of the steam bubbles were formed at the jet vortex ball leading edge. Here the droplet disengagement phenomenon at this region was the same as observed in the subcooled water tests, plus the addition of the steam bubbles. The bubbles coalesced and gradually rose to the surface in the region immediately surrounding the jet. Relatively little steam was visible being formed along the surface of the trailing column. For test #29 the jet-to-water ΔT was increased by a factor of two to 30C. There was also relatively little steam generation in this test, although greater than #19. By 0.2 s in this test the leading edge had penetrated well into the pool and the steam bubbles formed earlier had largely risen to the surface. Hence the camera views cleared, and it became evident in the closeup views of the trailing column that there was little steam generation along the column (as opposed to the leading edge), and furthermore that there was less surface irregularity and droplet disengagement along this vertical region than in the tests with subcooled water. Hence the appearance of a greater breakup length in tests 19 and 29 may be due to the small presence of a vapor region immediately surrounding the jet in those tests. Less disengagement of droplets from along the vertical column means there is a longer distance of the central high-velocity jet feeding material into the leading edge. Hence the leading edge breakup and heat transfer processes appear to be even more dominant during the initial jet flow stage for the condition of small net steam generation.

The behavior was dramatically different when the jet temperature was increased to 320C for test #13. The rate of steam generation was so great that by as early as 0.1 s the water pool was experiencing severe disruption. Steam that

was formed behind the leading edge essentially filled the entire vessel cross section and, in flowing upward, caused the equivalent of a massive pool boilup. The boilup itself disrupted the jet trailing column. The region was churn-turbulent with visible levitation of WM droplets. It is clear in this test that a certain mass of jet material had penetrated beyond the zone of disruption and that the remaining mass in the trailing column experienced abrupt and complete breakup as a result of the physical agitation. The relative masses could not be discerned in the motion pictures due to the observed vision in the high void region. Figure 4 shows that the leading edge penetrated to the limit of view at L/D = 30 without any indication of reaching a full breakup condition. Since there was a dispersal of the trailing column, it would have been anticipated that the leading edge would have been depleted early of its mass influx.

For test #24 the WM temperature was further increased to 455C. Although there was substantial steam generation, it was in no way comparable to test #13, suggesting that the boiling regime was beyond the nucleate boiling peak heat flux into the transition region or perhaps into film boiling. Most of the steam generated initially originated from the leading edge region with very little evident along the trailing column. A typically large volume of steam was left with the disengaged droplets in the wake region of the leading edge. Steam was continually formed at the leading edge as the jet progressed downward, leaving a long vertical steam region surrounding the trailing column. This prevented observation of the trailing column in the motion pictures except for the uppermost ten L/D's or so where there was no steam blanketing and also no significant amount of steam generation. Hence this test was consistent with others in the steam generation series in that the principal origin of the steam generation is the leading edge region and that relatively little takes place along the trailing column, albeit a steam blanket is left behind by the passage of the leading edge. The longevity of the central jet core feeding the leading edge is unclear in this test because, as typical, the motion picture view was obscured by the steam blanket, and the leading edge behavior in Fig. 4 lacks a clear break point.

The final set of tests utilized Cerrotru (CT) so that a debris bed of particles would be formed from the steam generation tests. A different injector with a larger melt mass was also used. Test #2 in this series ($T_{j,i}$ = 250C) was comparable in terms of steam generation to test #13 in the previous test. The steam generation occurred so rapidly that as early as 0.1 s the pool was undergoing vigorous agitation in a churn-turbulent flow regime. The jet trailing column was disrupted and there was visible levitation of droplets/particles. The particle bed consisted of both speherical particles of 3-5 mm diameter plus irregular filament formations of up to 20 mm across but typically very thin. The bed voidage measured in the as-settled state was 0.79. The jet penetration data in Fig. 5 shows a break from 4.0 to 1.9 m/s as early as L/D = 17 and a second break to 0.9 m/s at L/D = 40. The significance of a jet breakup distance per se in this test, as in #13, is largely lost due to the dominating effect of pool agitation in these cases.

The CT temperature was increased to 450C for JWM-5, comparable to the conditions of previous test #24. The observed steam generation behavior was very similar to that described for #24. Even the penetration behavior was similarly unclear, remaining approximately constant at 2 m/s over the observable length without a clear break point. A steam explosion was triggered in this test at 0.7 s, after material had begun to collect at the bottom. The trigger location was not located at the bottom but at L/D = 49. At that time there was relatively little steam below the trigger point, but there was a large steam blanket surrounding the jet above it. The pressure wave caused steam collapse with a propagation speed of 165 m/s. It was not apparent that any of the CT in the upper region

participated in the explosion; it may have been a purely local event. The explosion was not sufficiently energetic to do any damage to the Pyrex apparatus. Fine particles, coarse flakes, and spheres of 3-5 mm dia comprised the debris. Some of the spheres were hollow with very thin shells.

Test JWM-6 was a repeat of #5 with the temperature reduced to 400C. The test was qualitatively the same as #5 except there was no steam explosion. The leading edge penetration data lacked a clear break point as was the case for #5. One difficulty with the CT tests was that the larger injector tended to give a pour stream which was more irregular in size and tended to "wander" on exiting the delivery tube. Both these factors contributed to the somewhat irregular penetration behavior compared to the WM injector. From observation of the motion pictures, the best estimate of the breakup distance for tests JWM-5 and 6 is $L/D \tilde{=} 50$. The debris particles were essentially the same except for fewer fine fragments from #6.

MODEL EVALUATION

Jets can undergo various mechanisms of breakup depending on the conditions of injection. As the injection velocity is progressively increased four regimes of breakup have been described:[8]

1. Rayleigh regime - The jet undergoes axisymmetric oscillations destabilized by surface tension leading to breakup in the form of droplets.

2. Transition regime - The surface tension is augmented by the inertial force of the surrounding medium to accelerate the breakup process into drops in the order of the jet diameter.

3. Turbulent regime - Drops very much smaller than the jet diameter are formed by unstable growth of surface waves which are dependent on ambient conditions.

4. Atomization regime - Spray production from complete disruption of the liquid jet occurs at or very near the nozzle.

These regimes were derived from observations of small (millimeter) diameter jets of low density fluids. The ambient Weber number, We_a, based on the physical properties of the gas atmosphere is used as a criterion for the transition ($We_a > 0.4$) and turbulent regimes ($We_a > 1$). However, experimental data[9] for high density liquid metal jets depart significantly from these criteria,[9] and current experiments indicate that these criteria do not extrapolate well to large diameter jets.

Epstein and Fauske[6] considered the breakup of a jet blanketed by the vapor of liquid in which it is injected. They assumed a wave form for the jet, vapor, and liquid phases which resulted in six algebraic equations, each equivalent to zero, with six unknowns. They solved for the growth constant by setting the determinant equal to zero. The final derivations do not include surface tension which was employed in the initial pressure condition equations. In any case, for a thick vapor blanket (essentially infinitely thick) they obtained for the breakup length:

$$\frac{L_{jb}}{D_{j,i}} = \frac{\sqrt{3}}{2}\left(1 + \frac{\rho_v}{\rho_j}\right)\left(\frac{\rho_j}{\rho_v}\right)^{1/2}$$

For a very thin vapor blanket with thickness essentially equivalent to zero,

$$\frac{L_{jb}}{D_{j,i}} = \frac{\sqrt{3}}{2}\left(1 + \frac{\rho_\ell}{\rho_j}\right)\left(\frac{\rho_j}{\rho_\ell}\right)^{1/2},$$

where subscripts v and ℓ refer to the vapor and liquid phases.

Taylor[10] extended his analysis for the generation of ripples by wind blowing over a viscous fluid to the dispersion of liquid-metal jets in water. The length of the jet before breakup (system 1) was determined by comparison with existing data for jets and fluid atmospheres with different densities (system 2).

$$L_2 = L_1 \left(\frac{\rho_j}{\rho_f}\right)_2^{1/2} \Big/ \left(\frac{\rho_j}{\rho_f}\right)_1^{1/2}$$

Taylor used as a basis a breakup length of 150 jet diameters for a water jet in air and five jet diameters for a water jet in water which give essentially the same breakup lengths when applied to a system with a different jet density to ambient density ratio. He, therefore, determined a jet breakup length of 14 to 15 jet diameters for a liquid metal in water.

The Epstein and Fauske model and the Taylor model for jet breakup are shown in Fig. 6 as a function of the jet-to-ambient density ratio. Also shown on this figure are the data points from this study. The breakup lengths could not be determined for tests #13 and JWM-2 due to the vigorous pool boilup, nor for tests #7, 13, and 19 due to too short a camera viewfield, nor for test #23 where the jet fall occurred through air only. Among the remaining tests, the ambient fluid was assumed to be water for those performed with subcooled water and was assumed to be steam for tests with net vapor generation. The correctness of this latter assumption is highly in question, however, and the choice of appropriate ambient fluid density for the two-phase cases will require further examination. The measured breakup length in water of $L/D \sim 20$-25 is in reasonable agreement with the Taylor model, but exceeds the prediction of the E-F model by a factor of ~ 7. The best estimate breakup length in the vapor-dominated regime appears to agree more closely with the model of E-F, however.

It should be noted that core melt materials because of their very high temperature would produce a large amount of vapor, albeit in film boiling. The behavior would be more similar to tests #13 and JWM-2, which were found to be disrupted by the effects of the massive steam generation, rather than the low-temperature transition/film boiling cases of this study. As a consequence, it is unclear how extensive the breakup and quench process would actually be. The uncertainty arises because the breakup length would be expected to be very far in this boiling regime except that once under way, so much steam is generated that the trailing column(s) would be fragmented by the extreme agitation in the two-phase pool region. Further studies involving high-temperature corium melts are under way to address this, involving multiple as well as single pour streams.

ACKNOWLEDGEMENTS

This work was sponsored in part by the Electric Power Research Institute under contract RP1931-2 and by the U.S. Nuclear Regulatory Commission, FIN No. A2260-7. The assistance of technical managers M. Merilo and J. Telford at EPRI and NRC, respectively, is gratefully acknowledged. Figures were prepared by J. Kawka. The manuscript was prepared for publication by V. Eustace.

References:

1. B. W. Spencer, L. McUmber, D. Gregorash, R. Aeschlimann, and J. Sienicki, "Corium Quench in Deep Pool Mixing Experiments," ANS Proc, 1985 Natl Heat Transfer Conf, ANS #700101, Denver, CO, August 1985.

2. B. W. Spencer, J. D. Gabor, J. C. Cassulo, and D. J. Kilsdonk, "Results of Scoping Experiments on Melt Stream Breakup and Quench," Proc Intl ANS/ENS Topical Mtg on Thermal Reactor Saftey, ANS #700106, San Diego, CA, Feb 2-6, 1986.

3. B. W. Spencer, L. M. McUmber, J. J. Sienicki, and D. Squarer, "Results and Analysis of Reactor-Material Experiments on Ex-Vessel Corium Quench and Dispersal," Proc 5th Intl Mtg on Thermal Nuclear Reactor Safety, Karlsruhe, W. Ger., September 1984.

4. S. H. Han and S. G. Bankoff, "Film Boiling from a Vertical Jet of Fuel Entering a Water Pool," Nucl Eng and Des, 75, p. 81 (1982).

5. M. L. Corradini and G. A. Moses, "Limits to Fuel/Coolant Mixing," Nucl Sci and Engr, 90, p. 19 (1985).

6. M. Epstein and H. K. Fauske, "Steam Film Instability and the Mixing of Core-melt Jets and Water," ANS Proc, 1985 Natl Heat Transfer Conf, ANS #700101, Denver, CO, August 1985.

7. D. F. Hopkins and J. M. Robertson, "Two-dimensional Incompressible Fluid Jet Penetration," J. Fluid Mech, 29, pp 273-287 (1967).

8. R. D. Reitz, "Atomization and Other Breakup Regimes in a Liquid Jet," PhD Dissertation, Princeton U., Dept. Mechanical and Aerospace Eng., October 1978.

9. T. Ginsberg, "Liquid Jet Breakup Characterization with Application to Melt-Water Mixing," ANS Proc, 1985 Natl Heat Transfer Conf, ANS #700101, Denver, CO, August 1985.

10. G. I. Taylor, "The Dispersion of Jets of Metals at Low Melting Point in Water," The Scientific Papers of G. E. Taylor, Vol. III, Ed G. K. Batchelor, 1940.

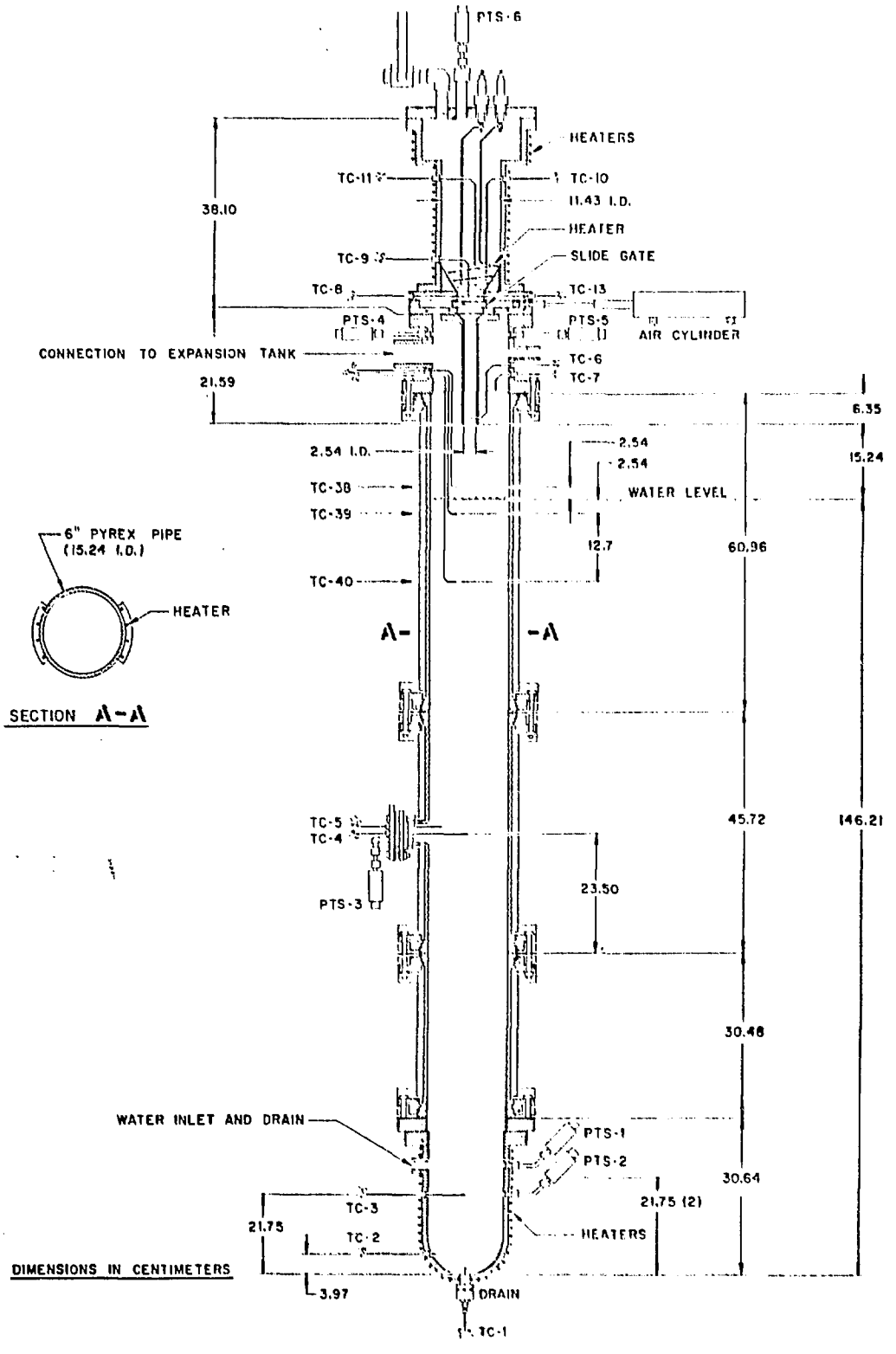

FIGURE 1. Jet mixing apparatus.

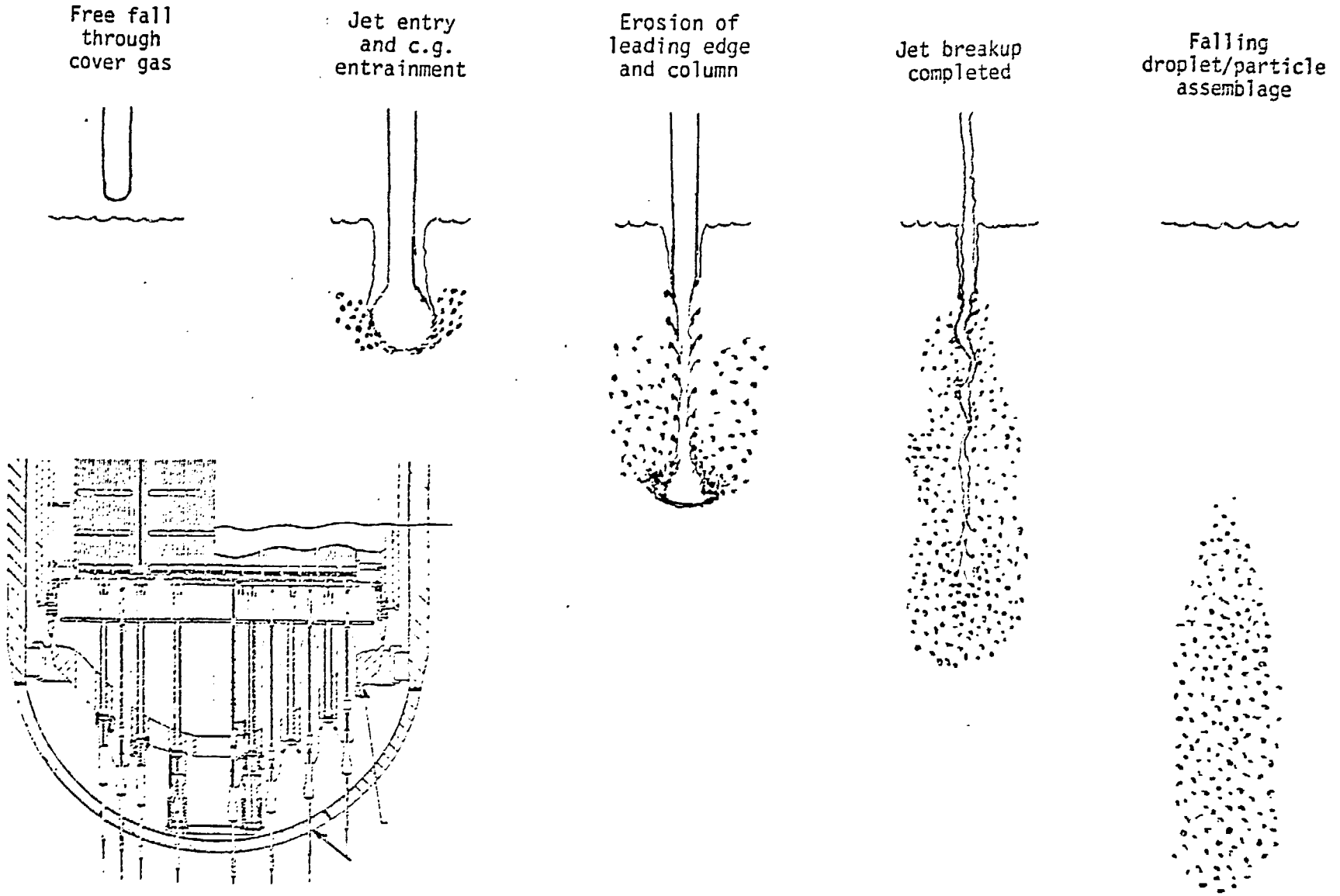

FIGURE 3. The breakup behavior of a corium stream draining through water in film boiling depends upon the water depth to jet diameter ratio, $L_w/D_{j,i}$.

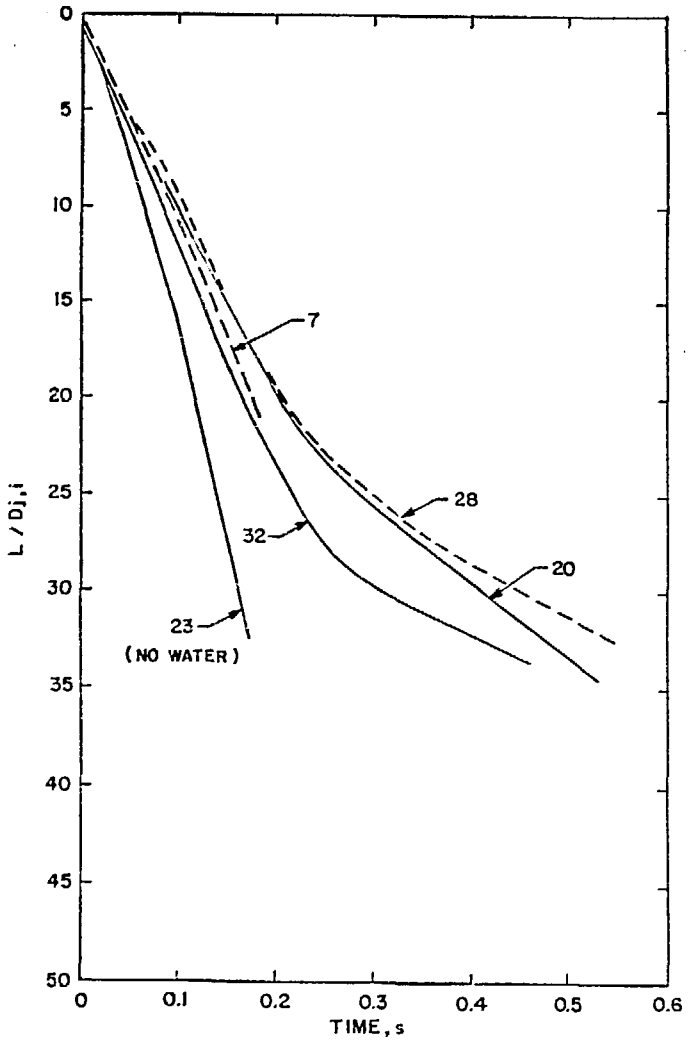

FIGURE 2. Jet leading edge penetration into water without net steam generation.

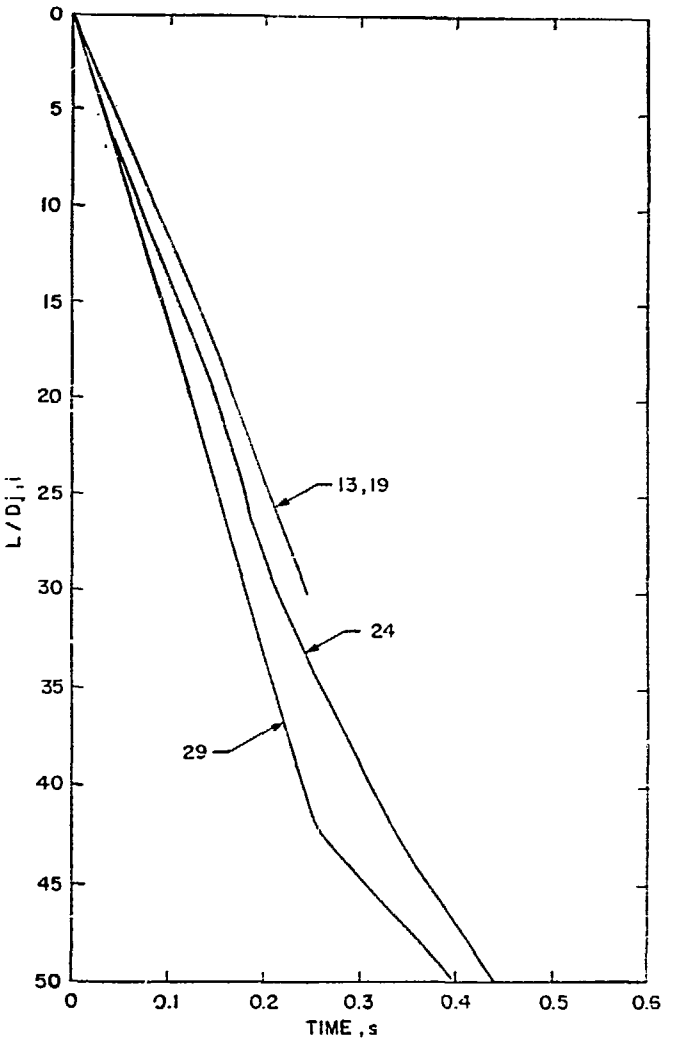

FIGURE 4. Jet leading edge penetration into water with net steam generation.

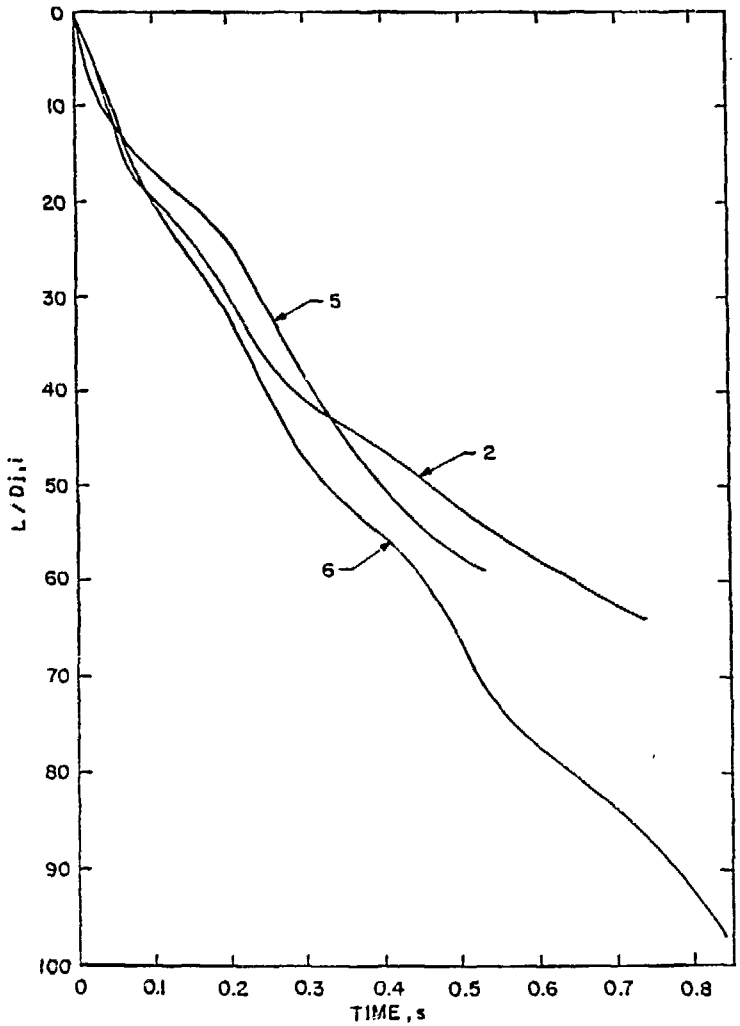

FIGURE 5. Leading edge penetration of Cerrotru jet into water with net steam generation.

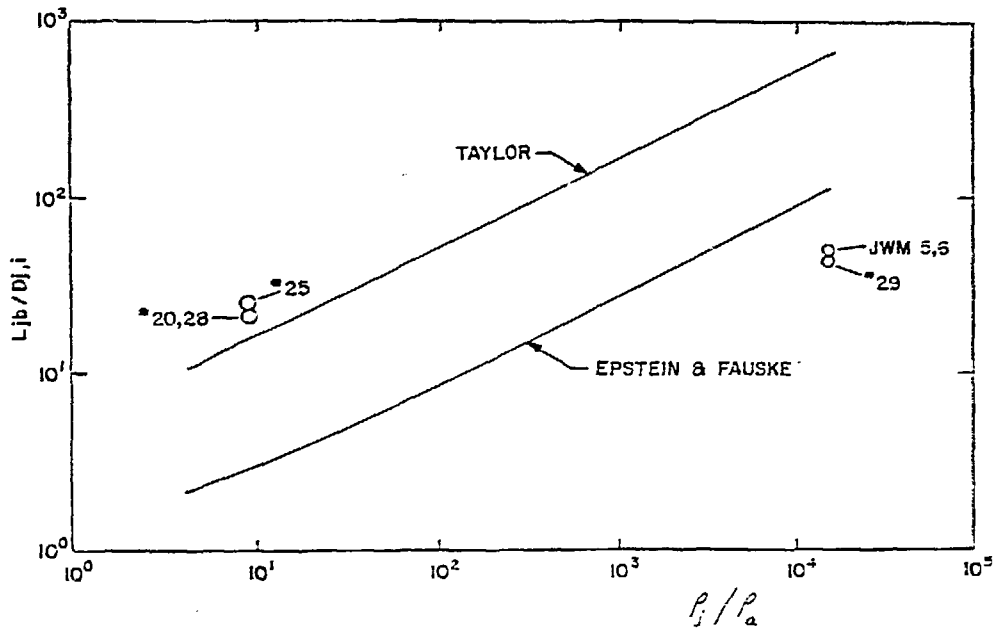

FIGURE 6. Jet breakup lengths compared with model predictions.